energies

MDPI

Article

A Novel Method for Diagnosing Power Electronics Devices Using Elastic Wave Emission

Maciej Kozak * and Radosław Gordon

Mechatronics and Electrotechnics Faculty, Maritime University of Szczecin, 70-500 Szczecin, Poland; r.gordon@pm.szczecin.pl
* Correspondence: m.kozak@pm.szczecin.pl

Abstract: This work is an introduction of acoustic emission (AE) signals used in order to detect the malfunction of selected semiconductor elements. The authors proposed the use of internally generated signals (elastic waves) of acoustic emission leading to the detection of the pre-fail state of switching IGBT transistors. The analysis of the AE signals allows the creation of a reference pattern of properly working transistors and at the same time the identification of abnormal signals, which are generated by a defective element. Unlike many papers, this article shows experimental results demonstrating a comparison of undamaged, properly working and defective IGBT transistors which can be used, for example, as a reference for diagnostic tools. Analysis of the signal in the frequency domain obtained from the faulty transistor (overheated or with damaged casing) shows the presence of additional frequencies which can indicate the imminent occurrence of critical damage.

Keywords: diagnostics; converters; IGBT transistors; acoustic emission

check for updates

Citation: Kozak, M.; Gordon, R. A Novel Method for Diagnosing Power Electronics Devices Using Elastic Wave Emission. *Energies* **2023**, *16*, 7405. https://doi.org/10.3390/en16217405

Academic Editor: Alon Kuperman

Received: 1 October 2023
Revised: 26 October 2023
Accepted: 29 October 2023
Published: 2 November 2023

Copyright: © 2023 by the authors. Licensee MDPI, Basel, Switzerland. This article is an open access article distributed under the terms and conditions of the Creative Commons Attribution (CC BY) license (https://creativecommons.org/licenses/by/4.0/).

1. Introduction

Modern electric machines are indispensable for the operation of marine vessels or, for example, so-called offshore drilling platforms or offshore wind farms. An important part of them are power electronics systems which gave designers and operators the opportunity to simplify and increase the efficiency of the mechanical part of the electric machine, but at the same time it complicated the control part. Currently, these are high-current circuits switched by a low-current and low-voltage microprocessor circuit.

Figure 1 shows an exemplary block diagram of a diesel–electric vessel. In addition to the drive, three propellers driven by an electric motor, there are also many devices that are controlled by semiconductor power devices called converters. The block diagram is not unambiguous; therefore, it can be assumed that the electric drive motors are powered and controlled by a voltage inverter-based system, which is made of high-power transistors. The converters can also be used in the line inverters generating the supply voltage, whose task is to maintain a constant voltage and power distribution on the supply rails. Converters are also used for feeding the electric machines driving, among others, centrifugal pumps, cargo and passenger lifts, bow thrusters and ventilation devices. All these converters are an important part of a power plant and are crucial for the safety of the ship. The authors proposed in [1] a new diagnostic method that allows to identify the state of a given switching semiconductor, using the analysis of the elastic wave generated in the semiconductor, which is strictly dependent on the changes occurring inside the semiconductor. The authors verified, among others, results obtained by a team of scientists, which were presented in [1].

A thorough analysis and research showed that the AE signals indicated in [2] came from a semiconductor element, but from a working power supply system. This fact may indicate that during diagnosing, special attention should be paid to the need to detect the emitted frequency band characteristic of individual modules, to use appropriate filters, and only in the next step to look for signals coming from a specific semiconductor element.

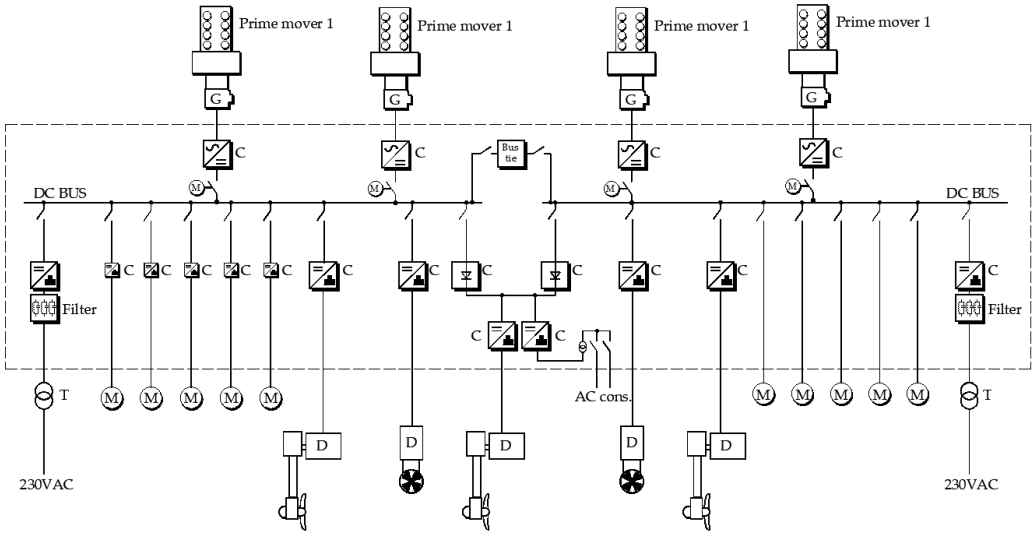


Figure 1. An exemplary electrical diagram of the diesel–electric vessel.

The issues of the failure rate of transistors and systems based on IGBT technology are identified by various research centers, but also by manufacturers and companies using them in their solutions and systems [3,4] through information reported directly by users as well as through active and passive experiments performed on exemplary laboratory systems or installed in industrial installations. Exemplary studies based on surveys [5] concerning requirements and expectations regarding the reliability of systems using IGBT structures showed that the failure rate was affected by several factors, including the following:

- The environment in which a given component operated (ambient temperature, humidity, salt content in the environment);
- Transients;
- Heavy loads;
- Switching frequency.

Figure 2 presents causes of failure of converter systems, developed on the basis of the literature [5].

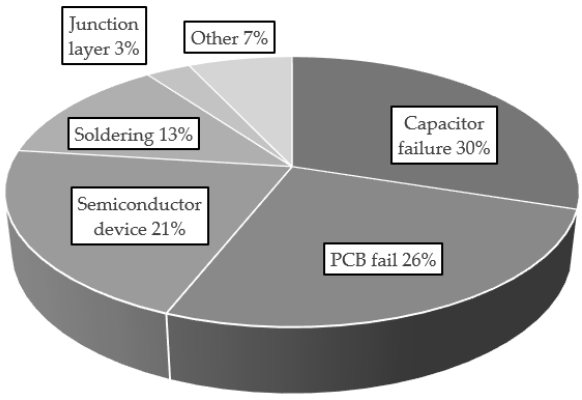


Figure 2. Various failures of switching semiconductor circuits.

The necessity to develop better, reliability-enhancing monitoring and control methods for the converter's operating parameters was noted in [6]. The authors of the research in [7,8], besides considering various electronic components, examined converter systems in which the main element was IGBT transistors. It was observed that over 50% of failures were caused by aging or damage to the IGBT module (or the transistor itself) or the capacitor. Traditionally, these cases can be observed through appropriate current or voltage measurements. The latest research is aimed at determining the state of the transistor in order

to detect potential damage before the complete immobilization of the system. Considering the failure statistics [5], it can be concluded that in every third case of malfunction, a semiconductor failure occurs.

The most common failure of a properly configured IGBT transistor is a failure in the connecting or internal junctions within the transistor itself. Such malfunctions can occur suddenly or, most often, undergo gradual degradation [9].

Methods that interfere with the structure of the system have the drawback of conducting measurements on a specially unprepared IGBT transistor circuit. In other work [10], a voltage measurement system was applied directly to the internal connecting wires within the studied component. A slightly different approach involves invasive methods (interfering with the circuit), as presented in [11]. In this case, the current flowing through the internal connecting wires of the circuit was measured by analyzing changes in the magnetic field generated by individual connections. These measurements were further developed in [12,13], where magnetic field sensors were integrated with the IGBT transistor.

On the other hand, non-invasive methods include those that do not interfere with the transistor's housing, thus enabling the measurement of various parameter changes without the need to attach additional measurement components/details inside the tested element. One of the utilized options is measuring the change in the IGBT gate charge [14,15]. Analyzing these and similar studies led the author to conclude that monitoring the capacitance charging time inside the transistor allows us not only to observe the time it accumulates charge but also that charging these capacitors can lead to the creation of an elastic wave. Since the authors in [15] demonstrate that the change in gate charge capacitance indicates the transistor's condition, the author of this work, based on analogy, assumed that the change in capacitance would affect the acoustic emission of the transistor and, therefore, it should be possible to identify the state of a given transistor without measuring the current. Similar to the work in [15], in [16], the measurement is related to the gate current value. It measures the gate capacitance charging time, which affects the transistor switching time. A change in this time can determine the transistor's state. Another parameter that can be measured to determine the condition of the connecting wires is checking the parasitic inductance of the IGBT gate [17]. Another method for detecting faults in connecting wires is measuring voltage at various points in the circuit, depending on the method, e.g., measuring the collector–emitter voltage in the on-state [4,18,19], and measuring current, such as proposed by the authors in [20], where the short-circuit current value is monitored. In general, it can be concluded that a decrease in the short-circuit current value is a sign of faults in the transistor connections.

According to [21], AE signal analysis is used as a tool for measurements of dynamic moduli, non-destructive testing (NDT) and for medical imaging. Another field of AE is the detection of elastic wave propagation in geology and mining. The acoustic emission sources generate signals which are useful in conditioning solid structures (cables, tanks, pressurized vessels, etc.). These signals can be related to cracking or rapid changes of inner structures caused, for example, by different thermal expand coefficients. It is worth noting that EA signals also prove useful in areas like current distribution panels, insulators and capacitors [22]. All these examples are linked to the influence ("interaction") of current on conductors and dielectrics. Ther are also some publications on the use of acoustic emission in various technical fields and its measurements allow authors to propose the utilization of elastic wave acoustic emission in diagnosing semiconductor components.

The literature regarding the utilization of AE signals [23], the reasons for their occurrence and the possibility of recording waves suggest that they can also be applied in the practical diagnosis of systems such as power electronic systems, high-voltage control systems or even individual elements directly related to their power supply.

As mentioned earlier, acoustic emission is increasingly used in the detection of defects in medium- and high-voltage transformers (insulation, breakdowns). This involves checking the condition of the insulation, with partial discharges identifying the degradation of insulating material [24–26].

In addition to the aforementioned optical fiber-based acoustic emission system, completely non-invasive systems based solely on piezoelectric transducers also exist [26].

Acoustic emission can also be used in diagnosing power insulators. An example is the research conducted by the authors of an article discussing the correlation between leakage current and measured acoustic emission [27,28].

2. Properties of Elastic Wave Propagation

In order to obtain an answer to the question regarding the possible use of elastic wave propagation and detection in solid materials including factors such as temperature, pressure or shape changes, the theoretical background and state of knowledge are presented in the following paragraph.

The rapid release of mechanical energy which propagates in the form of elastic waves from a certain point inside the solid structure or in a material is called acoustic emission. All the ways and methods leading to the recognition of the source of emission in the structures leading to the failure detection are also called acoustic emission. The propagation of elastic waves radiating from solid materials is caused by the release of energy in the form of waves generated in these regions. The sources of generated elastic waves can be indicated indirectly by analysis of the transient waves created in rapid processes with means of technology developed in the last 30 years.

The processes responsible for elastic wave generation inside the actual heterogeneous structures are very complex and there are different theories describing such phenomena. To simplify the analysis process, it is assumed to detect zones of microplastic deformation, emission sources can be represented as centers of deformation described by dynamic elastic theory [29] so the emission of waves and the propagation of generated signals in a wave then can be compared to the actual results obtained by measurements. As a matter of fact, there are serious problems with calculating AE, resulting in signals entirely from the information based on the input in an ideal system of a flat, glass plate because the surface response of such is mathematically difficult to evaluate [30]. Moreover, the exact measurement is always burdened with the uncertainty of the exact quantity piezoelectric sensor measures. In regular cases with means of AE, quantities such as displacement, velocity or amount of stress release can be measured. In the case under consideration, emissions generated in semiconductor devices are to be expected primarily from internal circuit displacement faults but all the aforementioned cannot be ruled out. To understand the nature of acoustic emission, the theoretical background of the sources of AE along with mathematical source functions of elastic waves can be presented.

The Navier–Cauchy equation describes the displacement field of the elastic waves at the spatial coordinate x and given time, so it can be stated, in other words, that this equation describes the movements inside a solid material in response to external forces and internal stresses.

The displacement field, $\vec{u}$, describes locations of the particles of the solid, by Newton's second law as follows:

$$\vec{f}\,\mathrm{d}V = \frac{\partial^2 \vec{u}}{\partial t^2}\mathrm{d}m = \rho\frac{\partial^2 \vec{u}}{\partial t^2}\mathrm{d}V \tag{1}$$

where dm is the particle's mass, dV is the particle's volume, ρ is the mass density and $\vec{f}$ denotes the force density.

To derive the Navier–Cauchy equation, Hooke's law should be included in Newton's second law, so Newton's law is as follows:

$$f_i + \sum\nolimits_j \nabla_j \sigma_{ij} = \rho\frac{\partial^2 u_i}{\partial t^2} \tag{2}$$

where $\nabla_j = \partial/\partial x_j$ is the partial derivative with respect to the j th coordinate.

The Hooke's law stress tensor $coefficients$ σ_{ij} equation is given by

$$\sigma_{ij} = 2\mu u_{ij} + \lambda\delta_{ij}\sum\nolimits_k u_{kk} \tag{3}$$

The components of the strain vector are defined by the following equation:

$$u_{ij} = \frac{1}{2}\left(\nabla_i u_j + \nabla_j u_i\right) \tag{4}$$

where u_i are the components of the displacement vector $\vec{u}$.

After inserting Equations (3) and (4) into Equation (2) and some rearrangement, we obtain the Navier–Cauchy equation in the form as follows:

$$\rho\frac{\partial^2 u_i}{\partial t^2} = f_i + \mu\sum_j \nabla_j^2 u_i + (\mu+\lambda)\nabla_i\sum_j \nabla_j u_j \tag{5}$$

where μ, λ are Lame constants of the medium.

The Equation (5) in the vector notation is referred as

$$(\mu+\lambda)\nabla(\nabla\cdot\vec{u}) + \mu\nabla^2\vec{u} - \rho\frac{\partial^2\vec{u}}{\partial t^2} = \vec{f} \tag{6}$$

The $\vec{f}$ force per unit mass (force density) generates the elastic wave in the material. The corresponding stress field tensor $\sigma(x,t)$ from (3) after considering isotropic tensor $\vec{I}$ can be expressed as

$$\sigma = 2\mu u_{ij} + \lambda\vec{I}\nabla\cdot\vec{u} + \mu(\nabla\vec{u} + \vec{u}\nabla) \tag{7}$$

If three perpendicular forces act at location x_0, the displacements are determined by a function $\vec{G}\left(\vec{x}-\vec{x}_0, t\right)$ that satisfies the dyadic equation given by

$$-\rho\vec{I}\,\delta\left(\vec{x}-\vec{x}_0\right)\cdot f(t) = (\lambda+\mu)\nabla^2\cdot\vec{G} + \mu\nabla^2\vec{G} - \rho\frac{\partial^2\vec{G}}{\partial t^2} \tag{8}$$

where $f(t)$ is an arbitrary scalar function described in time [30].

From Equation (8), the displacement field generated by other types of point sources, known from theory of elasticity can be derived.

In the case of the displacement caused by the current flow through an overheated semiconductor, a multi-layer structure based on the quoted theoretical description seems to be closest to the opening of the tensile crack inside the material. This can happen in the case of breaking bonding wires inside the transistor structure while switching operation under a high-junction temperature. When an acoustic wave is generated by a source in a certain volume, it is reflected multiple times by the bounding surfaces that form the wave guide. Due to the occurrence of the phenomenon of the interference of the reflected waves, the disturbance observed at a certain distance has a different character than one originating from the source. This phenomenon is known as the geometric dispersion of waves in a wave guide. From a practical point of view, to analyze wave propagation in different materials, a new Green's function should be derived for each of the waves in the wave guide. The algebraic solutions of such are presented for objects with quite simple geometrical shapes while more complex structures (including multi-layer volumes) are calculated with extensive use of numerical methods. Given the small size of the structures undergoing testing, such as IGBT transistors in TO-220 or slightly larger cases, there is no need for accurate internal fault positioning methods such as triangulation methods. It should be noted that the small size of the objects undergoing testing affects the multiplied reflection of waves from the boundary areas, which results in acoustic emission waves with a high harmonic content. In addition, it is necessary to take into account the heterogeneity of the structure of transistors and also the variety of materials from which they are built. The way the silicon structure is internally connected to the metal leads and the housing also plays an important role in the propagation of elastic waves in the structures, which makes

an accurate analysis of the phenomena very difficult to model. Due to these limitations, the current research is mainly focused on experimental studies, observations and analysis of results obtained in tests of real objects.

3. Methods of Diagnostic Identification with Use of AE Signals

The phenomenon of acoustic emission (AE) has been known for centuries, but it was only in the 1950s that it was described and cataloged as a physical phenomenon. Historically, it was more about its typically acoustic form (e.g., audible crackling when a certain mechanical stress threshold is exceeded). In the mid-20th century, however, the acoustic emission name began to be used and defined. There is a certain inconvenience in the name itself, as it was translated from English as "acoustic emission". For most people, including some scientists, it is associated with the audible band, i.e., between 20 Hz and 20 kHz. In its original meaning, this concept is much broader, mainly in the case of the generated elastic wave frequency band (from a fraction of a hertz to the order of megahertz). Modern AE measurements record elastic waves over a much wider bandwidth and are limited only by the attenuation of waves and the sensitivity of the sensors used in the measurements. A certain explanation for the acoustic emission name (not limited to the band of audible sounds) is the historical understanding of the phenomenon. In the past, the only "sensor" was the human ear. As an example, working miners were able to predict a collapse in the mine based on the sounds they heard. What they heard were the characteristic sounds of stamps breaking or the earth moving. What the miners recorded was within the limits of audible phenomena, but in fact, it was an overlap of various signals, which nowadays can be broken down into many components with higher and lower frequencies. Similarly, in ancient times, the quality of sulfur was assessed. Depending on the sounds emitted when pressing it, classification was made as to how "good" the mineral is. The phenomenon of acoustic emission itself is defined as the propagation of elastic waves in various media. It can also be stated, following the author of [31], that acoustic emission arises as a result of the release of energy stored inside an elastic medium. It is a dynamic change related to the local reconstruction of the structure of the tested material (or materials) and arises as a result of the release of energy-binding molecules by, for example, cracking, phase transformations and deformations. In most cases, we deal with several phenomena at the same time. In 2011, the non destructive testing standard [32] was adopted which defines acoustic emission as a physical phenomenon occurring in a material in which, as a result of a certain process, a decaying elastic wave is created [33]. This general definition takes into account all forms of excitations (also, e.g., medium flow or tribological processes taking place in friction nodes). We distinguish three basic types of acoustic emission: discrete type, continuous type and mixed type (Figure 3).

Discrete acoustic emission is characterized by a clear increase and decrease in the impulse signal. As a continuous signal, the beginning and end of the decay of an AE event cannot be directly and clearly distinguished (there is no clear rise and fall of the wave within many events). Often, the continuous type of emission is also called the noise form. The third type of acoustic emission is the composite of both previous signals, where both a noise form depending on the ongoing process (e.g., the flow of a medium in a pipeline) and a discrete form (e.g., generated by phenomena caused by additional sources of energy "packets" which can be clearly indicated).

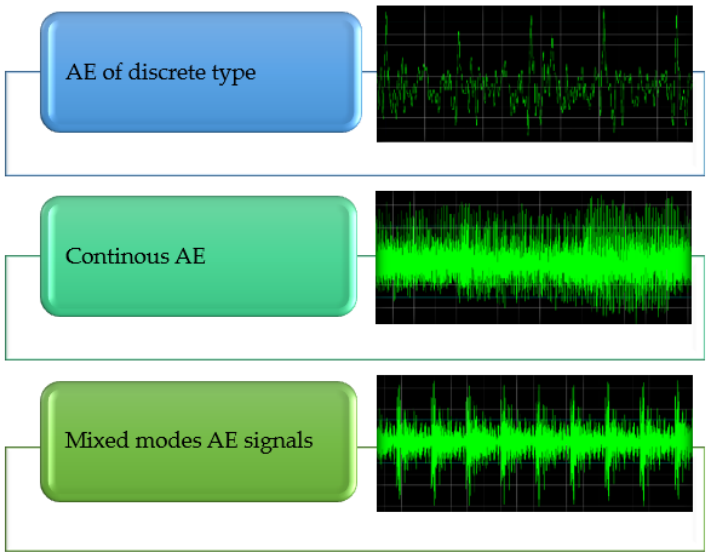


Figure 3. The types of acoustic emission signals.

4. Measures of AE Signals

The generated mechanical wave is subjected to physical phenomena. Figure 4 shows the basic physical quantities describing acoustic emission.

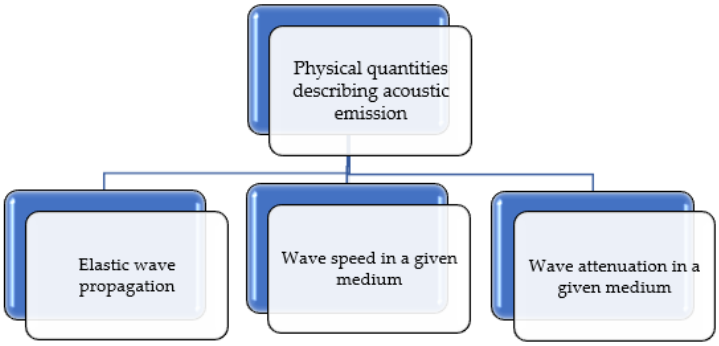


Figure 4. Physical quantities describing acoustic emission.

Characteristic wave properties can be pointed out as the following:

- Rectilinear wave propagation in homogeneous media;
- Reflection (at the boundary of media);
- Refraction (refraction);
- Diffraction;
- Interference;
- Beating;
- Splitting.

The mechanical wave in most media weakens, i.e., there is a gradual decrease in the amplitude, which is then an attenuation of the wave, which is caused by losses due to reflection, diffraction and scattering. When passing through an obstacle or a hole, the wave scatters or diffracts, i.e., diffraction occurring wave. If we distinguish between the phase and group speed of the wave, we are dealing with dispersion. Examples of dispersion curves for copper are shown in Figure 5.

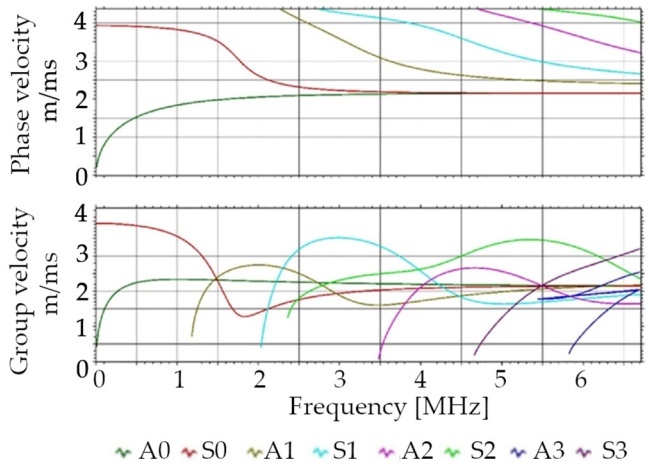


Figure 5. Dispersion curves for copper.

The movement of the envelope corresponds to group behavior, while the movement of zero crossings corresponds to phase behavior. Figure 6 shows the difference between group and phase velocities. The movement of the envelope corresponds to group behavior, while the movement of zero crossings corresponds to phase behavior.

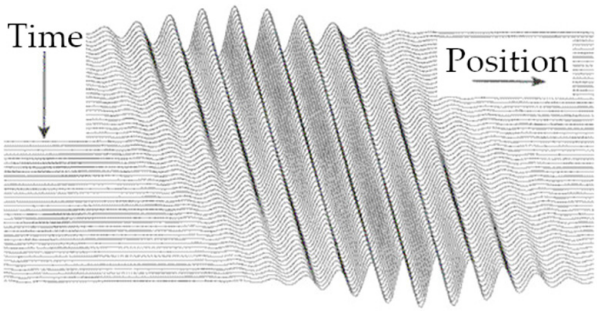


Figure 6. A characteristic showing the difference between group and phase velocities (wave envelope for a single carrier frequency).

Group velocity is the speed at which a wave moves through time and space. Therefore, it is the group velocity that interests us in diagnosing using the AE signal. Dispersion is caused by discontinuities or inhomogeneities in the medium in which the wave is moving. At the same time, it is a quite commonly used measure of the AE signal (especially in materials engineering), from which it is possible to draw conclusions about the characteristic frequencies of the propagating waves, and also to indirectly select a sensor with the appropriate frequency range of the measurement band. In a real medium, many phenomena act on the wave, which is why the concept of amplitude damping coefficient α [34] was introduced.

$$-\alpha dx = \frac{dA}{A} \tag{9}$$

After integration, we obtain

$$A = A_0 e^{-\alpha x} \tag{10}$$

where A is the amplitude of the elastic wave, dA depicts change in amplitude along the path dx and A_0 is the initial value of the amplitude $x = x_0 = 0$.

The decrease in amplitude with distance from the source is expressed by the minus sign in the formula. Attenuation also causes a decrease in energy with distance and is expressed by the energy attenuation coefficient γ and can be defined as follows:

$$-\gamma dx = \frac{dl}{I} \tag{11}$$

$$I = I_0 e^{-\gamma x} \tag{12}$$

where I is the intensity of the elastic wave, dl denotes change in intensity along the path dx and I_0 is the initial intensity value $x = x_0 = 0$.

As it is shown in the Equation (12), the decrease in intensity with distance from the source is expressed with a minus sign. Graphically, the attenuation can be represented as a decaying wave (Figure 7).

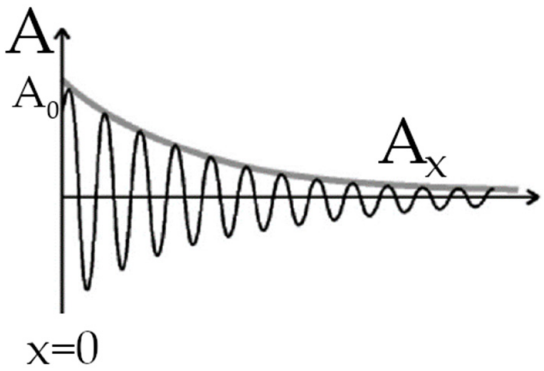


Figure 7. Visual representation of the wave absorption (attenuation) coefficient for an example amplitude from point $x = 0$ and the initial value A_0.

Due to their propagation, waves can be divided into the following

- Transverse waves have a direction perpendicular to the source surface and occur when a form of deformation is induced in the medium, e.g., in very viscous fluids or solids;
- Longitudinal waves created as a result of the movement of particles of the medium parallel to the direction of wave propagation; a change, i.e., deformation, in the volume of the medium then occurs;
- Stonley waves propagate at the boundary of two media;
- Lamb waves–plate waves, occurring in the so-called plates between two parallel surfaces;
- Love waves–transverse in layer systems, surface waves with the polarization of horizontal vibrations parallel to the layer, perpendicular to the direction of wave propagation;
- Rayleigh waves–surface–propagating on a free surface.

Wave motion practically disappears at a depth equal to the wavelength. Inside an elastic body, transverse and longitudinal waves usually propagate, which constitute a Rayleigh wave. Earthquakes are often a typical example of Rayleigh waves. The broad concept of an acoustic (mechanical) wave covers the full range of frequencies. From the order of a few per minute to hypersounds that are above 1 GHz, i.e., a period lasting nano- or even picoseconds (Table 1).

Table 1. Distinguishing acoustic waves based on frequency.

Name	Wave Frequency	Wave Cycle	Wave's Length in Vacuum
Hypersounds	Over 1 GHz	Below 10 ns	Shorter than 0.3 m
Ultrasounds	From 20 kHz up to 1 GHz	10 ns up to 0.05 ms	From 0.3 m up to 15 km
Audible frequency	From 16 Hz up to 20 kHz	0.05 ms up to 62.5 ms	From 15 km up to 19 km
Infrasound	Below 16 Hz	Over 62.5 ms	Over 19 km

The wavelength was given in a vacuum, but in other media, the wave propagates at a slower speed, which should be taken into account in numerous AE applications.

Considering that the above property of AE signals is important because depending on, e.g., the casing material, it should be taken into account in the selection of the tested descriptors and the construction of the appropriate measurement circuit. Acoustic emission signals can be used both in process research and in identifying the state of individual systems. It has a number of advantages, but there are also some limitations in terms of its practical application. Advantages of performing measurements/tests using acoustic emission are a follows:

- It can be a passive method;
- Does not require stopping production or decommissioning;
- Allows testing of the entire structure, also invisible and hidden parts;
- It is a dynamic measurement;
- Early detection of material damage (e.g., advancement of corrosion and often the place of its occurrence);
- Monitoring the condition of a given object.

There are certain limitations to acoustic emission diagnostic methods that should be remembered, including the following:

- The Kaiser effect (related to the fact that with the next load cycle not exceeding the previous value, acoustic emission should not occur [35]); hence, incorrect interpretations of the obtained test results may occur;
- The possibility of incorrectly stating the absence of damage when the AE signal does not change (e.g., if the crack does not widen);
- Lack of acoustic emission at constant load;
- Interference from surrounding devices and installations (mechanical and electromagnetic).

5. Acoustic Emission Descriptors

Acoustic emission sensors convert the mechanical wave into an analog electrical signal that varies in time and amplitude corresponding to this wave. It is therefore possible to directly observe changes in this signal, for example, on an oscilloscope. However, for AE flaw detection, ready-made devices are used which, depending on the application, "transform" the electrical signal into a form that can be described with the physical values.

The physical values depicted in the Figure 8 are defined as follows:

- The sum of threshold exceedances is obtained by counting the areas for which the amplitude exceeds the detection threshold;
- The sum of events during the measurement is the sum of all AE events registered in the measurement series (ΣN_{reg});
- The average value of the amplitude in a single measurement series, N_{avg}, is the quotient of the sums of acoustic emission events recorded in the measurement series to the number of measurement series.

The main signal descriptors of AE are visually presented in Figure 9 [35].

The processes causing acoustic emissions may include the following:

- Corrosion;
- Structure cracking;
- Phase transformations;
- Leaks;
- Cavitation;
- Partial discharges;
- Friction;
- Plastic and elastic deformation.

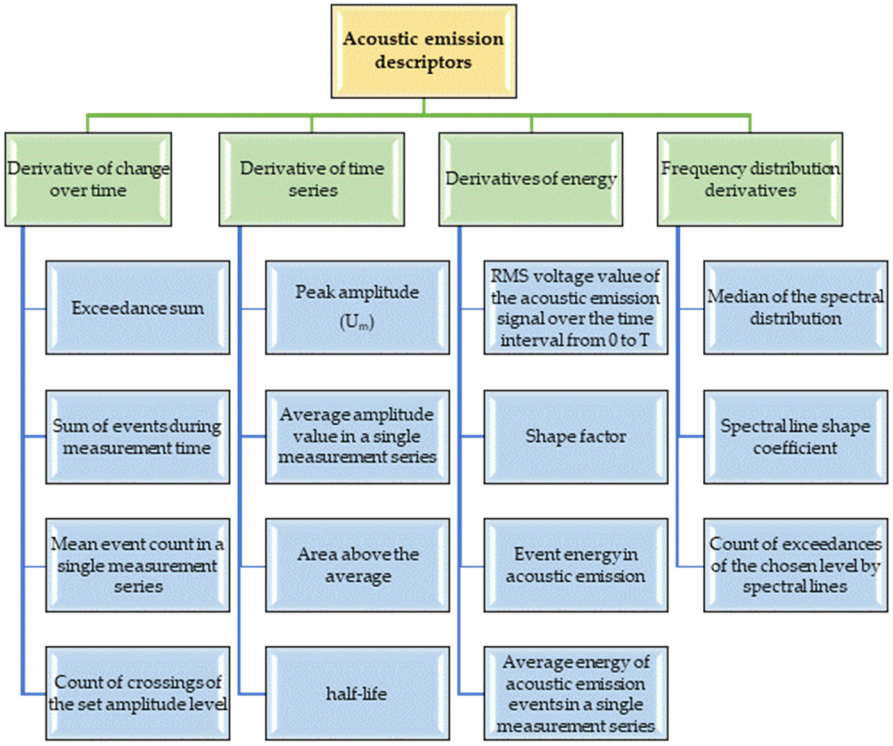


Figure 8. Acoustic emission descriptors classification.

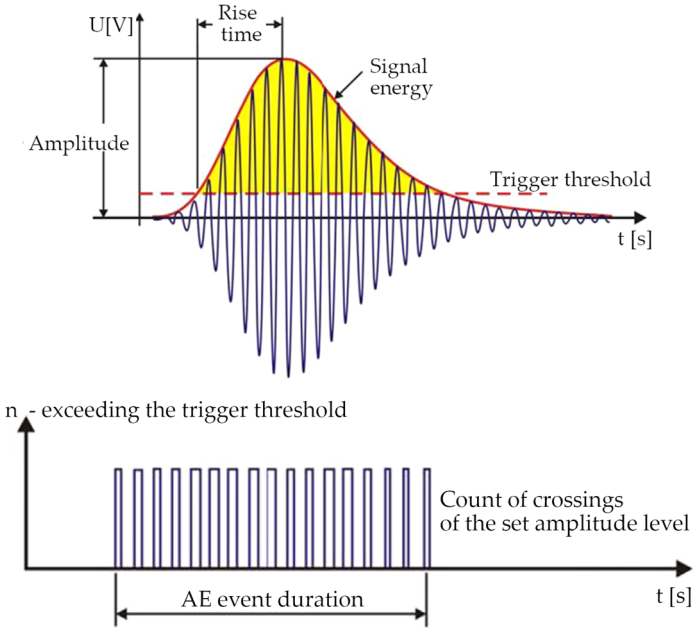


Figure 9. Visual representation of selected AE parameters.

6. Acoustic Emission Sensors

The piezoelectric effect is widely used in the equipment such as sensors, generators [36] or micro balancers. In the majority of the cases, acoustic emission sensors usually use the piezoelectric effect for measurement, i.e., a mechanical wave causes changes in the capacitance of the piezoelectric element, which in proportion to changes in the shape, generates changing voltage on the electrodes. Less popular are measurements using laser interferometers, which, despite their accuracy, are relatively expensive. An example of a laser sensor used in AE is, for example, a modified Michelson interferometer, where the sensor is an optical fiber and the generated elastic wave, causing deformation of the fiber,

changes the power of the light beam sent by the source. AE transducers are sensitive to the "surface movement" generated on the surface of the material to which they are attached. Fixed-frequency transducers, in a band close to their resonance frequency, are very sensitive, but within a narrow range that must be matched to the expected acoustic emission of the tested or observed object. This family of sensors records signals that occur primarily from 150 kHz to 300 kHz and are most commonly used in commercial applications. Another type of piezoelectric AE transducers are broadband sensors. Their disadvantage, however, is lower sensitivity (but the possibility of obtaining a wide bandwidth) and the need to use filters for specific applications. However, broadband sensors are useful, for example, for initial diagnostic tests, where it is not known what signal bandwidth can be expected. They are a kind of tool for selecting important bands of the diagnostic signal, which in the next step, can be narrowed down in combination with the selection of specific narrowband sensors [37]. For laboratory applications, one of the best solutions is the use of a laser interferometer. Its commercial applications are most often limited by the price of the device itself and the possible possibilities related to the skill (requires extensive knowledge) in the field of operation. Piezoelectric sensors work on the principle of the reverse piezoelectric effect, i.e., under the influence of deformation, electrical energy is generated between the electrodes. Sensors can have a simple structure, where the inverse piezoelectric effect is responsible for the so-called buzzer.

There may be a preamplifier built in the sensor housing which is externally powered by direct current. Signal separators are used to filter out the constant component. The most important element of such an acoustic sensor is a properly selected and formed piezoelectric element.

7. Experimental Results of AE Emission Signals of Damaged IGBT Transistor

In the following chapter, the results of acoustic emission tests of the switched transistor IXXH30N65 is presented. The study consisted of a comparative analysis of pre- and post-failure transistors by measuring acoustic emission under specific conditions. According to assumptions presented in Section 2, the IGBT transistors, with various levels of case damage and after thermal exposure, emit significantly more emission counts and the value of the energy of the acoustic emission event is much higher. The IXXH30N65 transistor was selected for the study for its number of switching operations in rated operating conditions. For the research, 10 transistors as seen in Figure 10 designated from T1 to T10 were used. These transistors were brand new and had not been used before where one of the important parameters of an IGBT transistor is the number of switches in nominal operating conditions.



Figure 10. The 10 IGBT transistors used in experimental research.

All transistors were subjected to acoustic emission testing on the laboratory test bench depicted in Figure 11 before and after purposely inflicting damage.

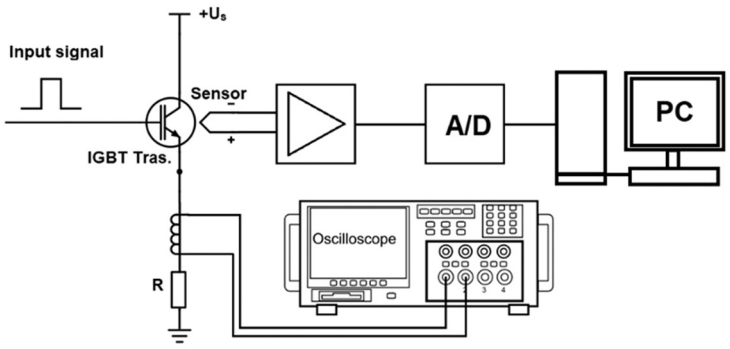


Figure 11. The scheme of the experimental setup used in the experimental tests.

For AE signal measurements, a proprietary device developed at the Maritime University of Szczecin, dedicated to measuring defects in fuel injection systems recording wave changes in acoustic emission, was used. This device was equipped with a high-pass input filter and an amplifier with adjustable gain. A PC equipped with an external signal converter from Creative Labs (Creative Technology Limited, Singapore) was used for recording, and the results were recorded using AudaCity software (3.3.1). The resulting files were saved in WAV format and then further processed using proprietary routines in the MATLAB environment and using SigView diagnostic software (6.2.3). Part of the analysis was conducted with use of the Visual AE software (R2021.1122) dedicated for AE analysis. Time and frequency domain charts were compared, as well as the frequency of registered acoustic emission counts.

Measurement parameters were fixed in the software, and the same parameter settings were used for comparisons. The VS150-M acoustic (Vallen Systeme, Wolfratshausen, Germany) emission sensor was mounted on the transistor's radiator. Another identical sensor was mounted on a separate metal plate to detect any disturbances in the measurement process and was configured in the same way as the testing main sensor. Appropriate measurement parameters (see Figure 12) were set in the LinWave 1002 distributed AE-System (Vallen Systeme, Wolfratshausen, Germany) which uses Visual AE software.

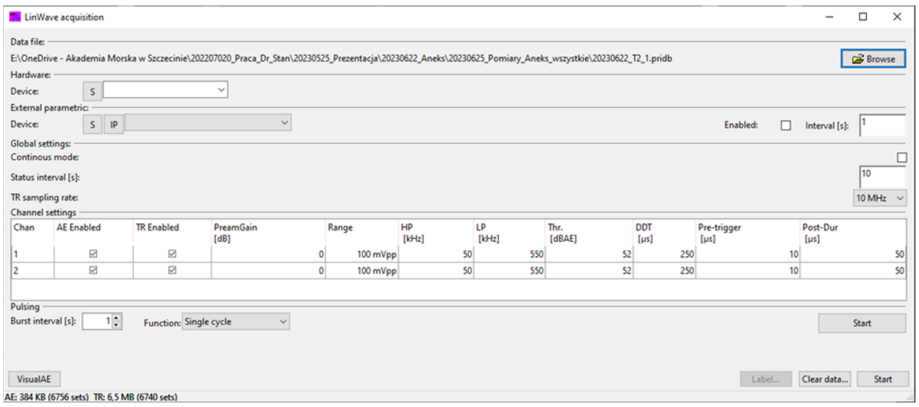


Figure 12. The measurement parameters set in LinWave 1002 compatible Visual AE software.

The bandpass filter was set to a slightly wider range than the sensor's passband, with a lower frequency of 50 kHz and an upper frequency of 550 kHz. The program recorded acoustic emission events above 50 dBAE and with a duration exceeding 250 us. Each event could be represented in the time domain as 10 us before the event and 50 us after the first count. These parameters were determined experimentally through a series of tests prior to the study.

The gate of the tested transistor was triggered by a voltage of 0 V and 15 V, at a frequency of 100 Hz. This frequency was obtained from a function generator, which generated a square wave voltage. The value of 15 V on the gate of the IGBT transistor was set by an operational amplifier operating as a comparator. This amplifier created electrical separation and allowed for the adjustment of the voltage offset, enabling output values ranging from −15 V to 15 V. The power supply voltage (applied to the transistor's CE junction and load resistance) was set to 15 V from a DC power supply.

The transistor's load consisted of a resistive wire wrapped in a ceramic framework with a suitably chosen resistance. The ambient temperature during transistor operation was at room temperature, ranging between 23 and 25 °C. Each measurement lasted from 60 to 120 s and was recorded in a separate file for further analysis. The table displays the average values of the current flowing in the conducting state through the collector–emitter junction. Various parameters were tested in the pre-test phase prior to the main investigation.

Transistor tests were conducted at various switching frequencies. The frequency was adjusted using a knob on the function generator, and measurements were obtained in the range from 8 Hz to 150 Hz and between 82 Hz and 1 kHz. As it turned out, the changes in switching frequency had a negligible impact on the acoustic emission of the tested transistors. As it was expected, the number of events varied depending on the switching, but these events did not differ significantly in the time domain. Tests were also conducted with different supply voltages, and the measurements showed changes in signal amplitude, but the plotted curves on the graphs were similar in both time and spectrum. The first stage involved checking the acoustic emission of each transistor under the aforementioned conditions. The measurement parameters were below the rated values, but acoustic emission signals were also detected on the radiator.

The T1–T10 transistors measurements were visually compared and found to differ from each other, but common characteristics could be distinguished. A characteristic frequency of acoustic emission was observed around 150 kHz and in each case, the new transistor had an acoustic emission of similar amplitude (about 0.1 mV). The differences in the recorded signals were influenced by many external factors, e.g., instability of the power supply voltage, temperature-induced changes in load resistance, varying transistor pressure on the radiator and differences in transistor manufacturing. The average current flow was measured for each undamaged transistor and after some mechanical and thermal induced damages and the values were summarized in the Table 2.

After conducting measurements with functional transistors, they were damaged in various ways. T1, T2 and T3 were mechanically manipulated to ensure that temperature did not affect the stresses in the housing. The remaining transistors were subjected to thermal stress at different temperatures starting from 200 °C. Transistor T1 was gradually drilled as it is presented in Figure 13, and after each hole was made, it underwent testing, with the results presented in the acquisition software compatible with LinWave 1002 distributed AE system.

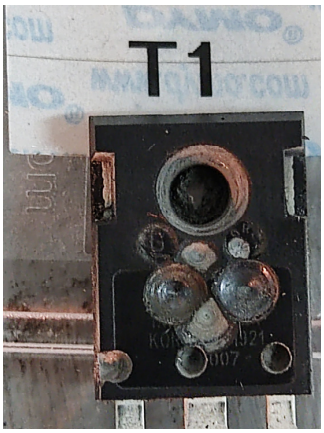


Figure 13. Drilled case of T1 transistor.

Table 2. Results of the average current flow through investigated IGBT transistors.

Transistor	Average Current Flow through Undamaged Transistor	Average Current Flow through Damaged Transistor	Sort of Damage
	[A]	[A]	
T1	5.02	5.03	Holes of 3.5 mm diameter drilled in the casing
T2	5.07	5.06	Mechanical compression
T3	5.06	-	Mechanical compression (total damage–not usable)
T4	5.00	4.95	Transistor heated to 350 °C for 10 min in a laboratory furnace
T5	4.94	4.88	Transistor heated to 350 °C for 5 min in a laboratory furnace
T6	4.95	4.87	Transistor heated to 370 °C for 5 min in a laboratory furnace
T7	5.15	4.95	Transistor heated to 340 °C for 10 min in a laboratory furnace
T8	5.16	4.92	Transistor heated to 340 °C for 5 min in a laboratory furnace
T9	5.20	5.28	Transistor heated to 320 °C for 10 min in a laboratory furnace
T10	5.05	5.04	Transistor heated to 250 °C for 15 min in a laboratory furnace

A sample lasting for at least 60 s was registered during transistor switching. The previously selected parameters for recording acoustic emission events allowed for the detection of events related solely to the transistor switching. Example of AE switching signals recordings is given in Figure 14, in which the undamaged IGBT transistor was examined.

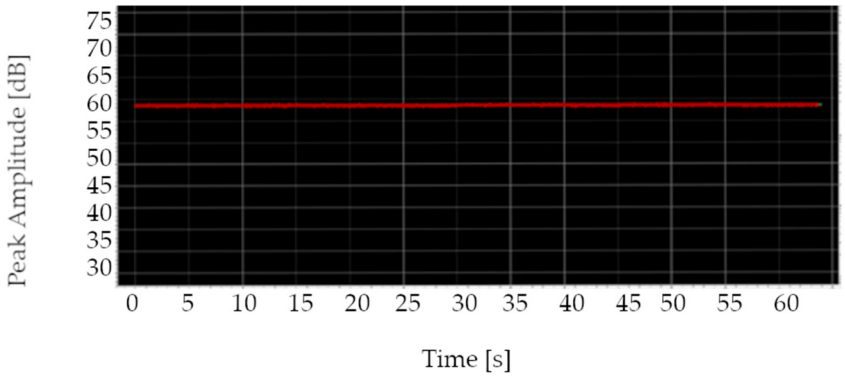


Figure 14. The emission of acoustic signals during the switching of transistor T1 recorded for a duration of 80 s at a frequency of 100 Hz.

In Figure 15, which is a one-second excerpt of a recording, it can be observed that the events are spaced approximately one-hundredth of a second apart, corresponding to the switching frequency. Different positions of points of acoustic emission events on the amplitude axis are caused by a significant approximation and imperfections in the equipment which can be contributed mainly to the fact that the power supply was of pulse type and a relatively small current flow could cause the transistor not to have enough time to discharge internal capacitances.

Each recording of acoustic events represented in Figure 15 by red dots can be presented in the time domain as well as in the frequency domain graphs, while in Figure 16 there is an example of AE signals obtained from brand, new IGBT. As it was observed, the events throughout the entire study period had very similar parameters.

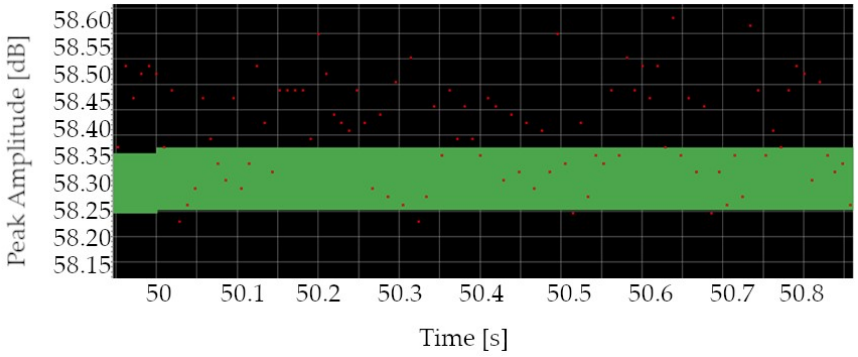


Figure 15. The waveform of the AE signals of transistor T1 switches.

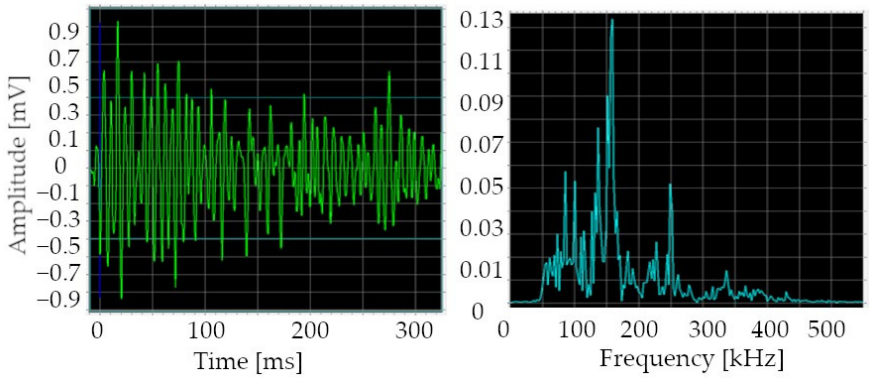


Figure 16. Single acoustic emission event of the new IGBT switch caused by transistor T1 switching.

After drilling holes in the transistor housing, as it is depicted in Figure 17, slight changes in characteristic frequencies were observed regardless of the type of damage, confirming that AE wave is emitted during switching. In the 140–160 kHz band, the amplitudes of the signals had similar levels, but the frequencies themselves shifted slightly.

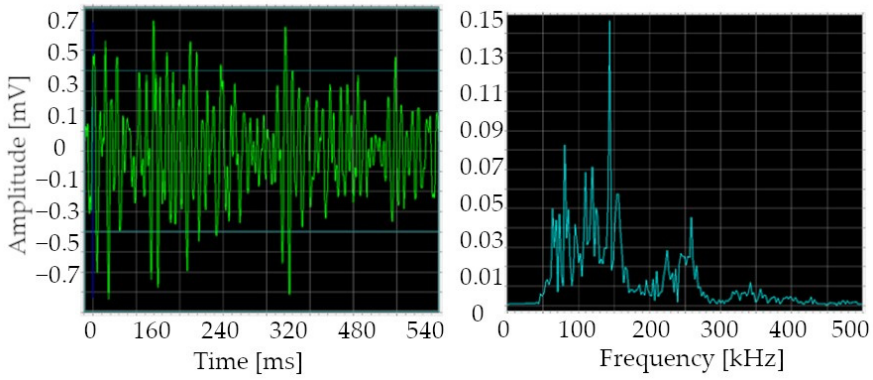


Figure 17. Single acoustic emission event of a T1 transistor with damaged case (drilled holes).

In the next test, the transistor denoted as T2 was also subjected to mechanical compression and its housing was significantly damaged (see Figure 18), but the transistor was still able to switch the current flow.

On the oscilloscope-acquired waveform, the changes in flowing current were negligible, and the 0.1 A decrease in current was insignificant and has been credited to measured noise.

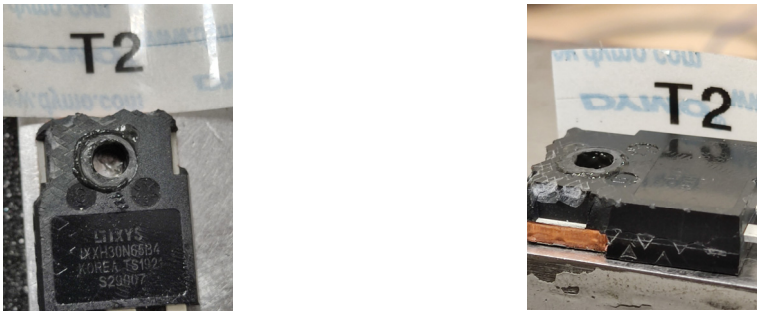


Figure 18. The appearance of a mechanically damaged transistor T2.

However, a significant increase in acoustic emission events or counts was observed what can be noted by comparison of upper and lower waveforms in Figure 19. When the trigger threshold was shifted to 55 dBAE, only transistor switching was noted.

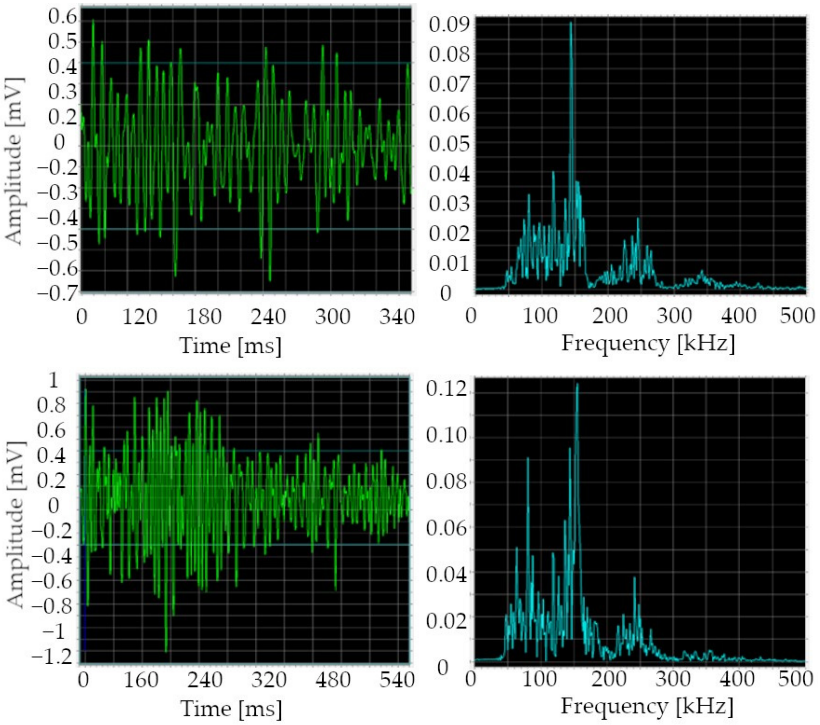


Figure 19. Single acoustic emission event waveform of the brand new transistor T2 (upper) and the mechanically stressed IGBT (lower).

8. Discussion

The changes in chassis stress cause changes in acoustic emission, but they are negligible in this case. The changes made to the chassis structure were insignificant to the transistor's operation. The T2 test results show that partial disintegration of the transistor housing resulted in a significant increase in acoustic emission events over the entire tested band. On the other hand, suppression of some frequencies in the 140–160 kHz band and amplification of others was observed. A higher amplitude of frequency striations in the 50–100 kHz range was also noted. Damage to the housing results in the generation of other frequencies, as in the case of a new transistor. The transistors T4–T10 were exposed to temperatures ranging from 280 to 350 °C and with different heating periods. The T10 transistor was exposed to a temperature of 280 °C for a period of 15 min. The temperature of 300 °C is the limit for soldering this transistor in up to 10 s, while the operating temperature was a maximum of 175 °C and the overheating effects was visible in the acoustic emission profile. There was a significant increase in acoustic emission events during switching and unidentified events

above the set trigger threshold, i.e., 52 dBAE which can be seen by comparative analysis of the AE events waveforms in the Figures 20 and 21. For comparison, the trigger threshold was changed to 56 dBAE. When comparing the waveforms with changed parameters, it can be clearly observed that acoustic emission occurs in similar frequency bands, but these frequencies differ significantly in amplitude.

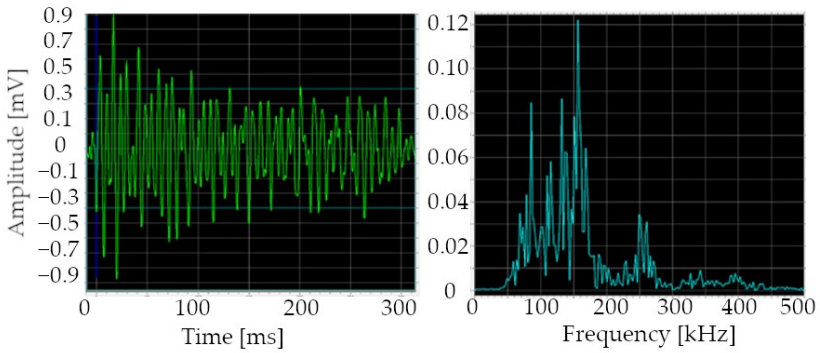


Figure 20. A single acoustic emission event of a brand new transistor.

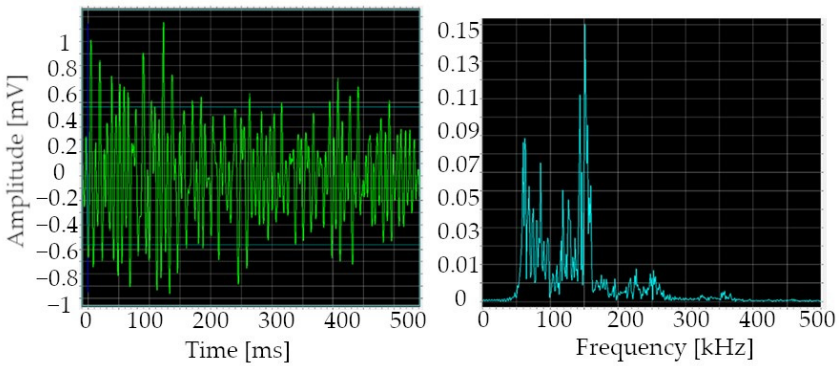


Figure 21. A single acoustic emission event of a transistor heated up to 280 °C.

9. Conclusions

Damage to the housing causes changes in the observed frequencies and amplitudes of the signals received from the sensor. Therefore, the recorded signals came from elements related to the casing and the influences on its temperature changes are caused by the failure of the cooling system. One of the causes of acoustic emission may be the failed or loose connections between the semiconductor and the leads. They conduct significant current values in a short time while switching, and are affected by the electromagnetic field and the change in length caused by thermal expansion. Changing the shape and structure of the housing resulted in different displacements of these connections, and therefore, different acoustic emissions. If the recorded emission corresponds to mechanical changes in these connections, it can be determined whether a given connection emits a changed elastic wave by observing these changes. The altered elastic wave emitted by the semiconductor terminals delivers information that the critical damage to the semiconductor-printed circuit board connection may be imminent. Such damage is statistically one of the most common causes of damage to a power electronics element or the entire module.

The following conclusions can be drawn from the literature analysis and our own research:

1. During operation, the IGBT emits an elastic wave of acoustic emission.
2. Internal phenomena occurring in the IGBT transistor generate the formation of an elastic wave AE.
3. Using AE elastic waves, the state of the tested transistor can be identified.

4. There are characteristic and repeatable AE wave frequencies for each properly operating (switching) transistor.
5. A change in charge in the semiconductor generates an acoustic emission signal.
6. An increase in the temperature of the semiconductor system causes a decrease in the amplitude of AE signals (visible) in the low-band frequency.
7. "Partial" damage to a semiconductor system generates an increase in AE events.
8. In the case of a properly functioning transistor, the acoustic emission of switching is repeatable.
9. Regardless of the type (design solutions) of IGBT transistors, the acoustic emission signals generated by them have common features related to, for example, the signal related to switching or an increase in the transistor temperature.
10. Piezoelectric sensors used in AE research are sensitive to external magnetic fields.
11. As observed, the changes in the amplitude and frequency content of acoustic emission signals were dependent on the type of damage. It can be concluded that for the type of transistor tested, the amplitude of the signals emitted by the switching transistor was at the same level than that obtained from the overheated transistor (see Figures 20 and 21). By comparing the results, there is a difference in the content of higher harmonics for the overheated IGBT.

The conclusion is that proposed diagnostics using acoustic emission can be successfully used to describe the pending damage to devices operating in the marine environment. At the stage of ongoing research, the relationship between acoustic emission signals and the exact type of damage to the semiconductor structure of IGBT transistors is being sought.

Author Contributions: Conceptualization, M.K. and R.G.; methodology, R.G.; software, M.K.; validation, R.G. and M.K.; formal analysis, M.K.; investigation, M.K. and R.G.; resources, R.G.; data curation, R.G.; writing—original draft preparation, M.K.; writing—review and editing, M.K.; visualization, R.G.; supervision, M.K.; project administration, M.K. and R.G.; funding acquisition, M.K. and R.G. All authors have read and agreed to the published version of the manuscript.

Funding: This research received no external funding.

Data Availability Statement: No data available for public use.

Conflicts of Interest: The authors declare no conflict of interest.

References

1. Kärkkäinen, T.J.; Talvitie, J.P.; Kuisma, M.; Hannonen, J.; Ström, J.P.; Mengotti, E.; Silventoinen, P. Acoustic emission in power semiconductor modules—First observations. *IEEE Trans. Power Electron.* **2014**, *29*, 6081–6086. [CrossRef]
2. Błachowicz, A. Zastosowanie Modelowania 3-D w Diagnostyce Kondensatorów Elektroenergetycznych Wykonywanej Metodą Emisji Akustycznej. Ph.D. Thesis, Uniwersytet Opolski, Opole, Poland, 2014. Available online: https://9lib.org/document/9ynelwly-zastosowanie-modelowania-diagnostyce-kondensatorow-elektroenergetycznych-wykonywanej-metoda-akustycznej.html (accessed on 1 September 2023).
3. Sikorski, W.; Walczak, K. Power transformer diagnostics based on acoustic emission method. *Acoust. Emiss.-Res. Appl.* **2013**, *1*, 1–13. [CrossRef]
4. Singh, A.; Anurag, A.; Anand, S. Evaluation of Vce at inflection point for monitoring bond wire degradation in discrete packaged IGBTs. *IEEE Trans. Power Electron.* **2017**, *32*, 2481–2484. [CrossRef]
5. Wolfgang, E. *Examples for Failures in Power Electronics Systems, Presented at ECPE Tutorial on Reliability of Power Electronic Systems*; European Center for Power Electronics e.V.: Nuremberg, Germany, 2007; Volume 16, pp. 1–5.
6. Yang, S.; Xiang, D.; Bryant, A.; Mawby, P.; Ran, L.; Tavner, P. Condition monitoring for device reliability in power electronic converters: A review. *IEEE Trans. Power Electron.* **2010**, *25*, 2734–2752. [CrossRef]
7. Choi, U.M.; Blaabjerg, F.; Iannuzzo, F. Advanced power cycler with intelligent monitoring strategy of IGBT module under test. *Microelectron. Reliab.* **2017**, *76*, 522–526. [CrossRef]
8. Aryan, P.; Sampath, S.; Sohn, H. An overview of non-destructive testing methods for integrated circuit packaging inspection. *Sensors* **2018**, *18*, 1981. [CrossRef]
9. Luo, D.; Chen, M.; Lai, W.; Xia, H.; Deng, Z.; Wang, Z.; Yu, K. A Fault Detection Method of IGBT Bond Wire Fatigue Based on the Reduction of Measured Heatsink Thermal Resistance. *Electronics* **2022**, *11*, 1021. [CrossRef]

10. Lehmann, J.; Netzel, M.; Herzer, R.; Szcześniak, P. Method for electrical detection of bond wire lift-off for power semiconductors. In Proceedings of the ISPSD'03. 2003 IEEE 15th International Symposium on Power Semiconductor Devices and Ics, Cambridge, UK, 14–17 April 2003; pp. 333–336. [CrossRef]
11. Shiratsuchi, H.; Matsushita, K.; Omura, I. IGBT chip current imaging system by scanning local magnetic field. *Microelectron. Reliab.* **2013**, *53*, 1409–1412. [CrossRef]
12. Tomonaga, H.; Tsukuda, M.; Okoda, S.; Noda, R.; Tashiro, K.; Omura, I. 16-Channel micro magnetic flux sensor array for IGBT current distribution measurement. *Microelectron. Reliab.* **2015**, *55*, 1357–1362. [CrossRef]
13. Sheng, M.; Alvi, M.H.; Lorenz, R.D. Real-time Bond Wire Lift-off Monitoring via Module Integrated Current Sensors. In Proceedings of the 2019 IEEE Energy Conversion Congress and Exposition (ECCE), Baltimore, MD, USA, 29 September 2019–3 October 2019; pp. 3163–3169.
14. Zhou, S.; Zhou, L.; Sun, P. Monitoring potential defects in an IGBT module based on dynamic changes of the gate current. *IEEE Trans. Power Electron.* **2013**, *28*, 1479–1487. [CrossRef]
15. Davari, P.; Kristensen, O.; Iannuzzo, F. Investigation of acoustic emission as a non-invasive method for detection of power semiconductor aging. *Microelectron. Reliab.* **2018**, *88*, 545–549. [CrossRef]
16. Wang, K.; Zhou, L.; Sun, P.; Du, X. Monitoring bond wires fatigue of multichip IGBT module using time duration of the gate charge. *IEEE Trans. Power Electron.* **2020**, *36*, 888–897. [CrossRef]
17. Zhang, Q.; Yang, Y.; Zhang, P. A novel method for monitoring the junction temperature of SiC MOSFET on-line based on on-state resistance. In Proceedings of the 2019 22nd International Conference on Electrical Machines and Systems (ICEMS), Harbin, China, 11–14 August 2019; pp. 1–5.
18. Choi, U.M.; Blaabjerg, F. Separation of wear-out failure modes of IGBT modules in grid-connected inverter systems. *IEEE Trans. Power Electron.* **2017**, *33*, 6217–6223. [CrossRef]
19. Du, M.; Kong, Q.; Ouyang, Z.; Wei, K.; Hurley, W.G. Strategy for diagnosing the aging of an IGBT module by on-state voltage separation. *IEEE Trans. Electron Devices* **2019**, *66*, 4858–4864. [CrossRef]
20. Sun, P.; Gong, C.; Du, X.; Luo, Q.; Wang, H.; Zhou, L. Online condition monitoring for both IGBT module and DC-link capacitor of power converter based on short-circuit current simultaneously. *IEEE Trans. Ind. Electron.* **2017**, *64*, 3662–3671. [CrossRef]
21. Walley, S.M.; Field, J.E. *Reference Module in Materials Science and Materials Engineering. Elastic Wave Propagation in Materials*; Elsevier: Amsterdam, The Netherlands, 2016. [CrossRef]
22. Wotzka, D. Modelowanie Sygnałów Emisji Akustycznej Generowanej Przez Wybrane Klasy Wyładowań Niezupełnych. Ph.D. Thesis, Uniwersytet Opolski, Opole, Poland, 2010.
23. Wang, L.; Wang, H.; Wang, L.; Lü, H.; Ning, W.; Jia, S.; Wu, J. Experimental investigation of transient earth voltage and acoustic emission measurements of partial discharge signals in medium-voltage switchgears. In Proceedings of the 2013 2nd International Conference on Electric Power Equipment-Switching Technology (ICEPE-ST), Matsue, Japan, 20–23 October 2013; pp. 1–4. [CrossRef]
24. Kuo, C.C.; Tsao, T.F. A novel defect classification system of cast-resin transformers by neural network under acoustic emission signal. In Proceedings of the 6th WSEAS International Conference on Instrument, Measurement, Circuits & Systems, Hangzhou, China, 15-17 April 2007; pp. 93–98.
25. Búa-Núñez, I.; Posada-Román, J.E.; Rubio-Serrano, J.; Garcia-Souto, J.A. Instrumentation system for location of partial discharges using acoustic detection with piezoelectric transducers and optical fiber sensors. *IEEE Trans. Instrum. Meas.* **2014**, *63*, 1002–1013. [CrossRef]
26. Kuo, C.C. Artificial recognition system for defective types of transformers by acoustic emission. *Expert Syst. Appl.* **2009**, *36*, 10304–10311. [CrossRef]
27. Li, H.; Wen, X.; Shu, N.; Pei, C. Application of Acoustic Emission Technol-ogy on Monitoring of Polluted Insulator Discharge. In Proceedings of the 2009 Asia-Pacific Power and Energy Engineering Conference, Wuhan, China, 27–31 March 2009; pp. 1–4. [CrossRef]
28. Álvarez-Nasrallah, B.; Candelo-Becerra, J.E.; Soto-Ortiz, J.D.; Pombo-Acevedo, J.; Díaz-Aparicio, O. Correlation analysis between ceramic insulator pollution and acoustic emissions. *TecnoLógicas* **2015**, *18*, 101–108. [CrossRef]
29. Love, A.E.H. *A Treatise on the Mathematical Theory of Elasticity*, 4th ed.; Dover Publication: New York, NY, USA, 1944.
30. Yih-Hsing, P. Theory of acoustic emission. In *Transactions of the Twenty-Sixth Conference of Army Mathematicians*; U.S. Army Research Office: Adelphi, MD, USA, 1981; pp. 389–396.
31. Malecki, I.; Opilski, A. Charakterystyka i klasyfikacja sygnałów EA. In *Emisja Akustyczna, Źródła. Metody. Zastosowania*; Wyd. Biuro PASCAL: Warszawa, Poland, 1994; pp. 35–52.
32. *EN 13554:2011-04*; Non-Destructive Testing—Acoustic Emission Testing—General Principles. Deutsches Institut für Normung, DIN: Berlin, Germany, 2011.
33. Śliwiński, A. *Ultradźwięki i Ich Zastosowanie*, 2nd ed.; Wydawnictwa Naukowo-Techniczne, WNT: Warszawa, Poland, 2000.
34. Łapiński, Z.; Łukaszewicz, J. Badanie metodą emisji akustycznej normalizowanych, hartowanych i wodorowanych próbek stalowych z karbem, podczas prób rozciągania. Efekt Kaisera. *Probl. Tech. Uzbroj.* **2006**, *35*, 129–142.
35. Caesarendra, W.; Kosasih, B.; Tieu, A.K.; Zhu, H.; Moodie, C.A.; Zhu, Q. Acoustic emission-based condition monitoring methods: Review and application for low speed slew bearing. *Mech. Syst. Signal Process.* **2015**, *72*, 134–159. [CrossRef]

36. Wang, F.; Zhao, X.; Guo, H.; Tian, Y.; Zhang, D. Design, modeling and experiment of a novel ultrasonic elliptical vibration generator. *Sens. Actuators A Phys.* **2023**, *363*, 114707. [CrossRef]
37. Keprt, J. Method of Acoustic Emission Sensor Calibration. 2005. Available online: https://www.fekt.vut.cz/conf/EEICT/archiv/sborniky/EEICT_2005_sbornik/03-Doktorske_projekty/03-Kybernetika_a_automatizace/05-xkeprt01.pdf (accessed on 1 September 2023).

Disclaimer/Publisher's Note: The statements, opinions and data contained in all publications are solely those of the individual author(s) and contributor(s) and not of MDPI and/or the editor(s). MDPI and/or the editor(s) disclaim responsibility for any injury to people or property resulting from any ideas, methods, instructions or products referred to in the content.